Supporting Information

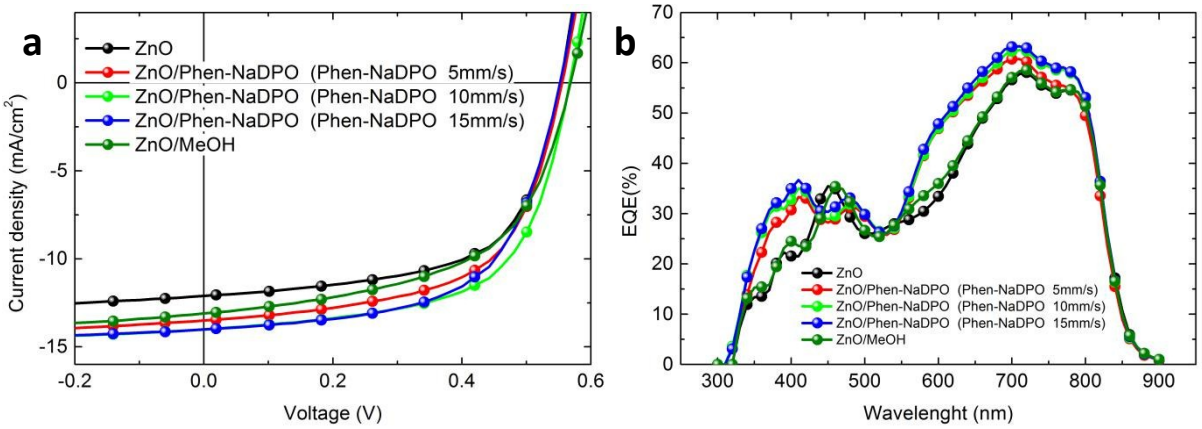

Figure S1. a) *j-V* characteristics of inverted OSCs with a different thickness of **Phen-NaDPO** coated onto ZnO and under simulated AM1.5 illumination (100 mW/cm^2); Methanol was doctor-bladed on top of ZnO as reference. b) EQE spectra of the inverted OSCs corresponding to (a).

Table S1. Summary of the *j-V* characteristics of inverted OSCs with differently thick **Phen-NaDPO** layers (doctor-blading speed: 5-15 mm/s) under simulated AM1.5 illumination (100 mW/cm^2); Methanol was doctor-bladed on top of the ZnO as reference.[a]

Devices configuration	V_{OC} (V)	J_{SC} (mA cm^{-2})	*FF* (%)	*PCE* (%) avg (best)
ZnO	0.56	-12.12±0.56	59.59±0.50	4.00 (4.30)
ZnO/**Phen-NaDPO** (5mm/s)	0.56	-13.56±1.07	59.04±1.56	4.48 (4.87)
ZnO/**Phen-NaDPO** (10mm/s)	0.56	-13.94±0.99	61.60±1.03	4.80 (5.08)
ZnO/**Phen-NaDPO** (15mm/s)	0.56	-14.19±0.46	59.75±0.95	4.75 (4.96)
ZnO/MeOH	0.56	-13.26±0.28	56.45±1.14	4.19 (4.30)

[a] Each value represents the average from five cells.

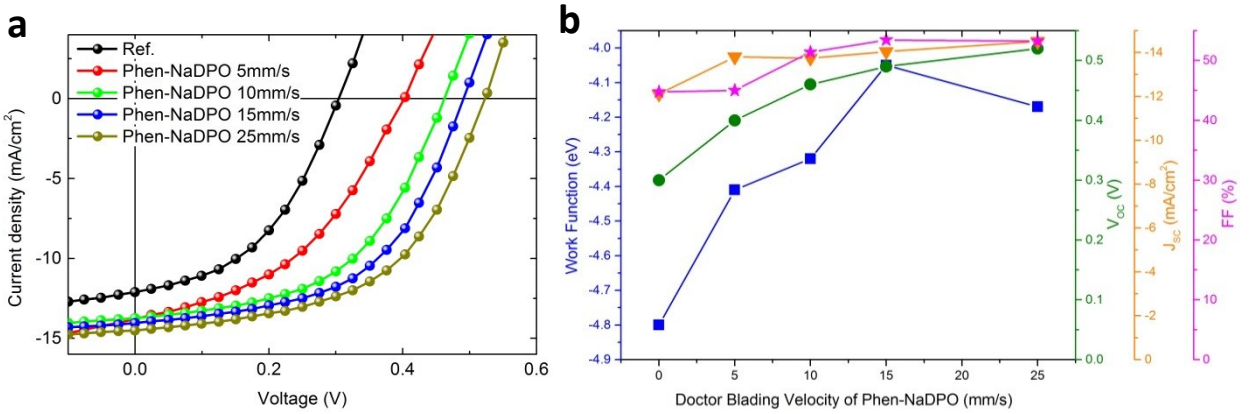

Figure S2. a) j-V characteristics of the organic solar cells (ITO/Phen-NaDPO/pDPP5T-2:PC61BM/MoO_3/Ag) with a different thickness of **Phen-NaDPO** under simulated AM 1.5G illumination (100 mW/cm^2). b) Corresponding photovoltaic parameters as a function of the work function for the different **Phen-NaDPO** layer thickness.

Table S2. Kelvin Probe Measurements of the Work Function of various substrates w or w/o **Phen-NaDPO**.[a]

Samples	Work function (eV)
ITO	–4.80 ± 0.03
ITO/ Phen-NaDPO (**5mm/s**)	–4.51 ± 0.01
ITO/ Phen-NaDPO (**10mm/s**)	–4.32 ± 0.03
ITO/ Phen-NaDPO (**15mm/s**)	–4.01 ± 0.03
ITO/ Phen-NaDPO (**25mm/s**)	–4.17 ± 0.01
ITO/AZO	–4.40 ± 0.01
ITO/AZO/ Phen-NaDPO (**15mm/s**)	–3.92 ± 0.02
ITO/ZnO	–4.26 ± 0.01
ITO/ZnO/Phen-NaDPO (**15mm/s**)	–3.83 ± 0.02

[a] The thicknesses of the AZO and ZnO are 50 and 50 nm, respectively; the thickness of deposited **Phen-NaDPO** film is also affected by the doctor-blading velocity from 5mm/s to 25 mm/s.

ITO/pDPP5T-2:$PC_{61}BM$:Phen-NaDPO/MoO_3/Ag

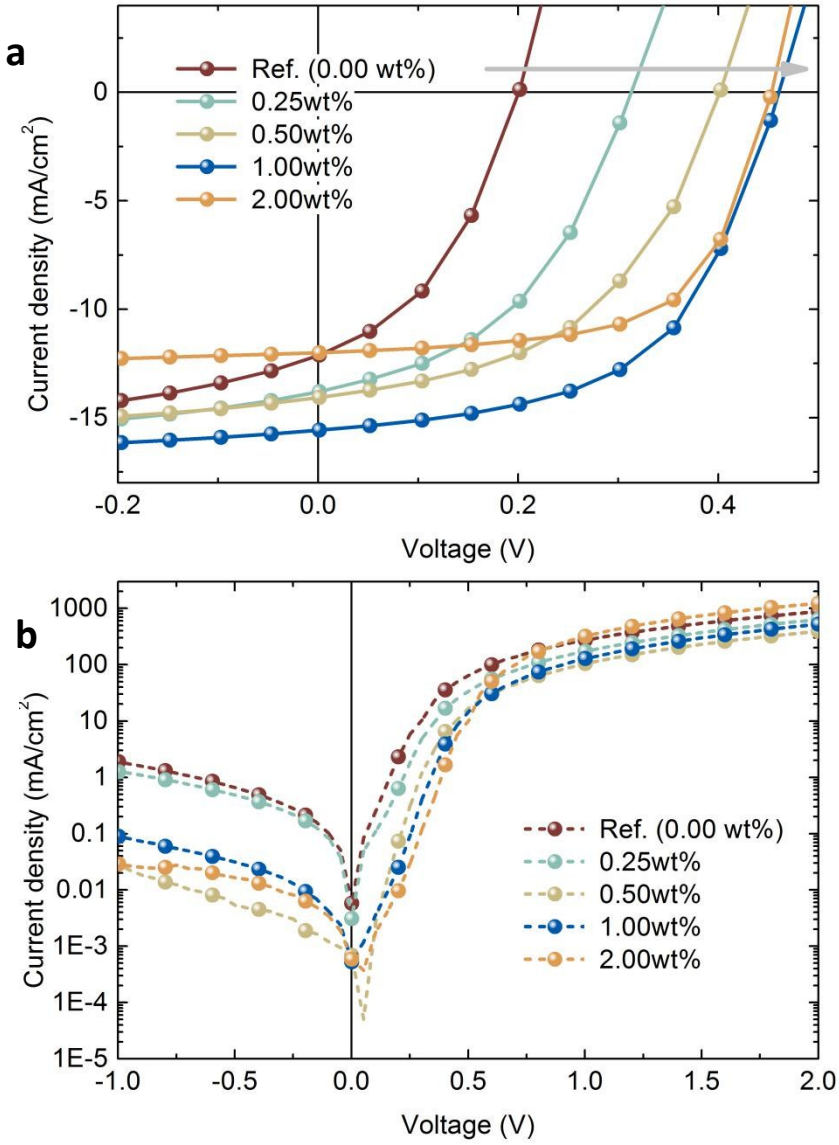

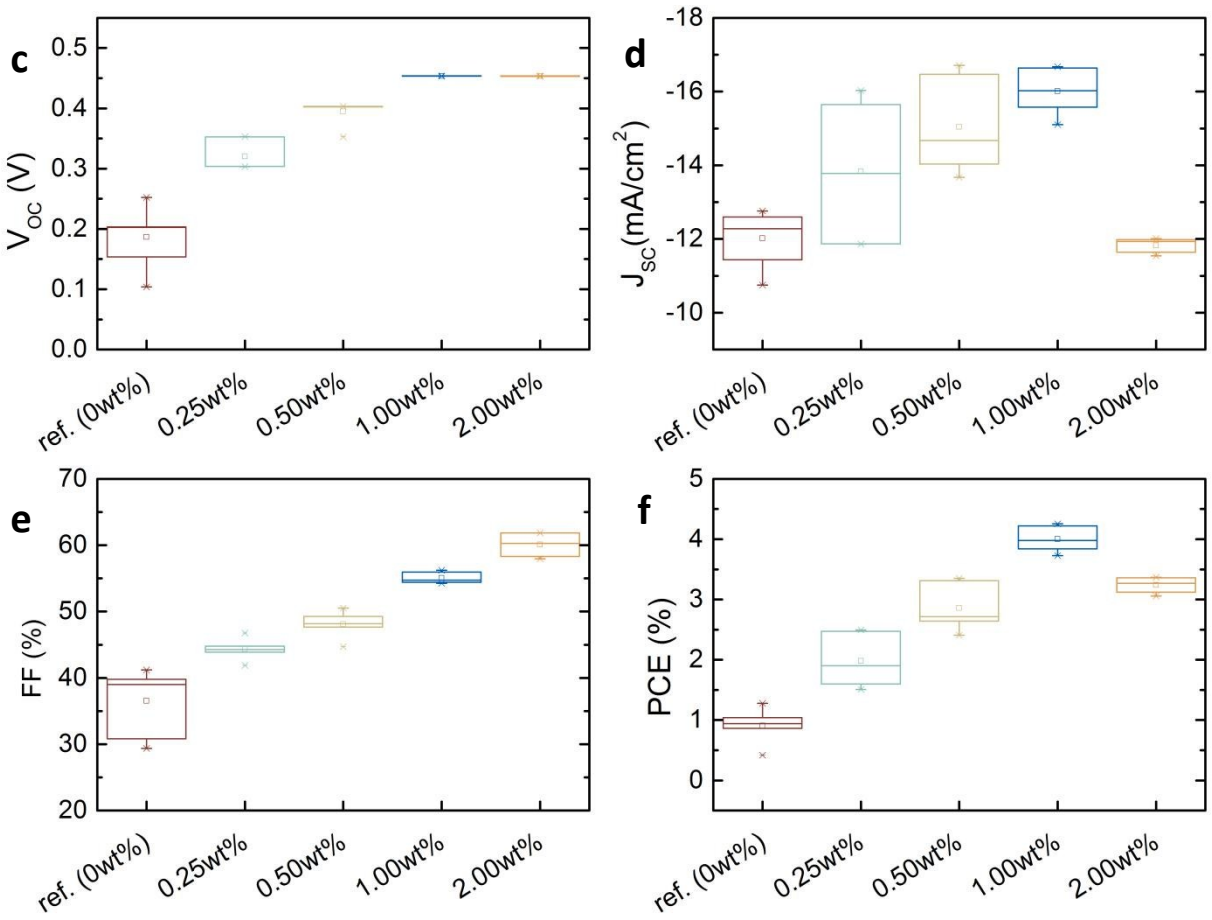

Figure S3. a) *j-V* characteristics of the OSCs (ITO/pDPP5T-2:$PC_{61}BM$:**Phen-NaDPO**/MoO_3/Ag) with different **Phen-NaDPO** contents in the ternary blend under illumination of an AM 1.5G solar simulator (100 mW/cm^2). b) Corresponding logarithmic plot of dark *j-V* characteristics. C-f) Photovoltaic parameters distribution of 5 solar cells; the boxes represent the 25-75% distribution range, and hollow squares represent the mean values.

ITO/AZO/pDPP5T-2:$PC_{61}BM$:Phen-NaDPO/MoO_3/Ag

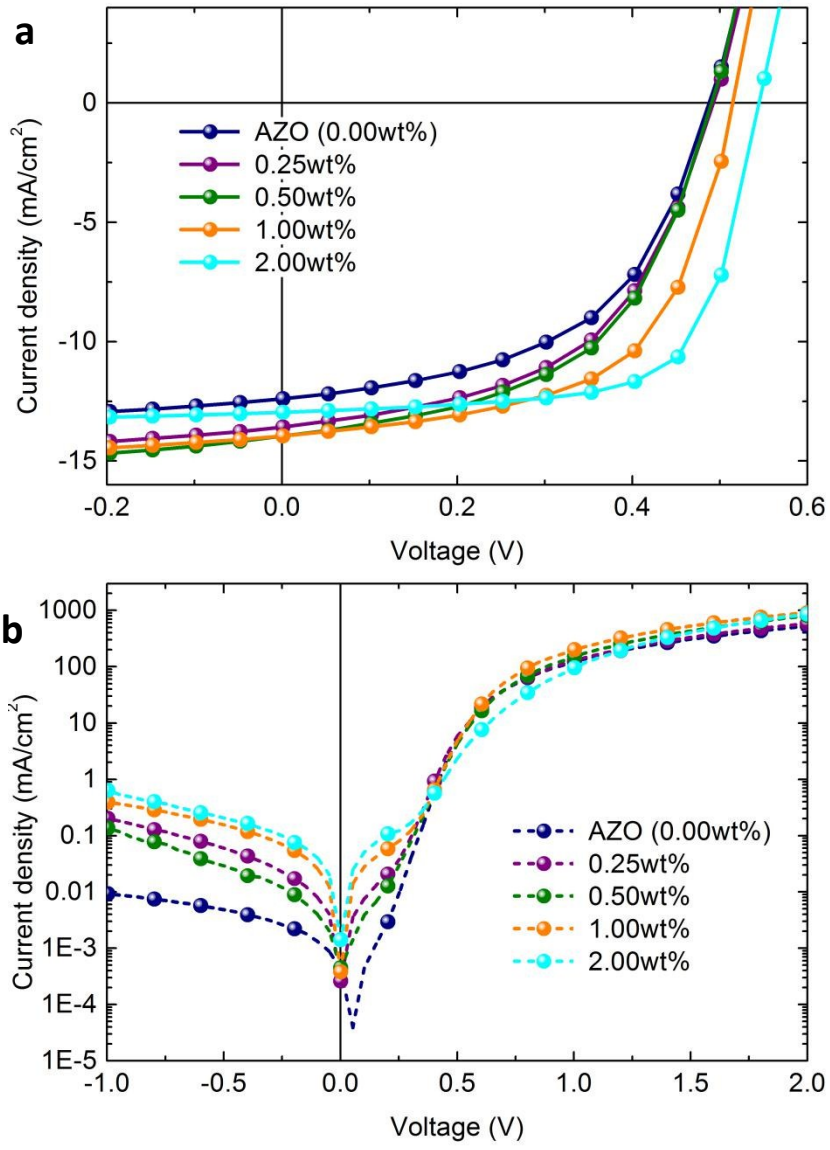

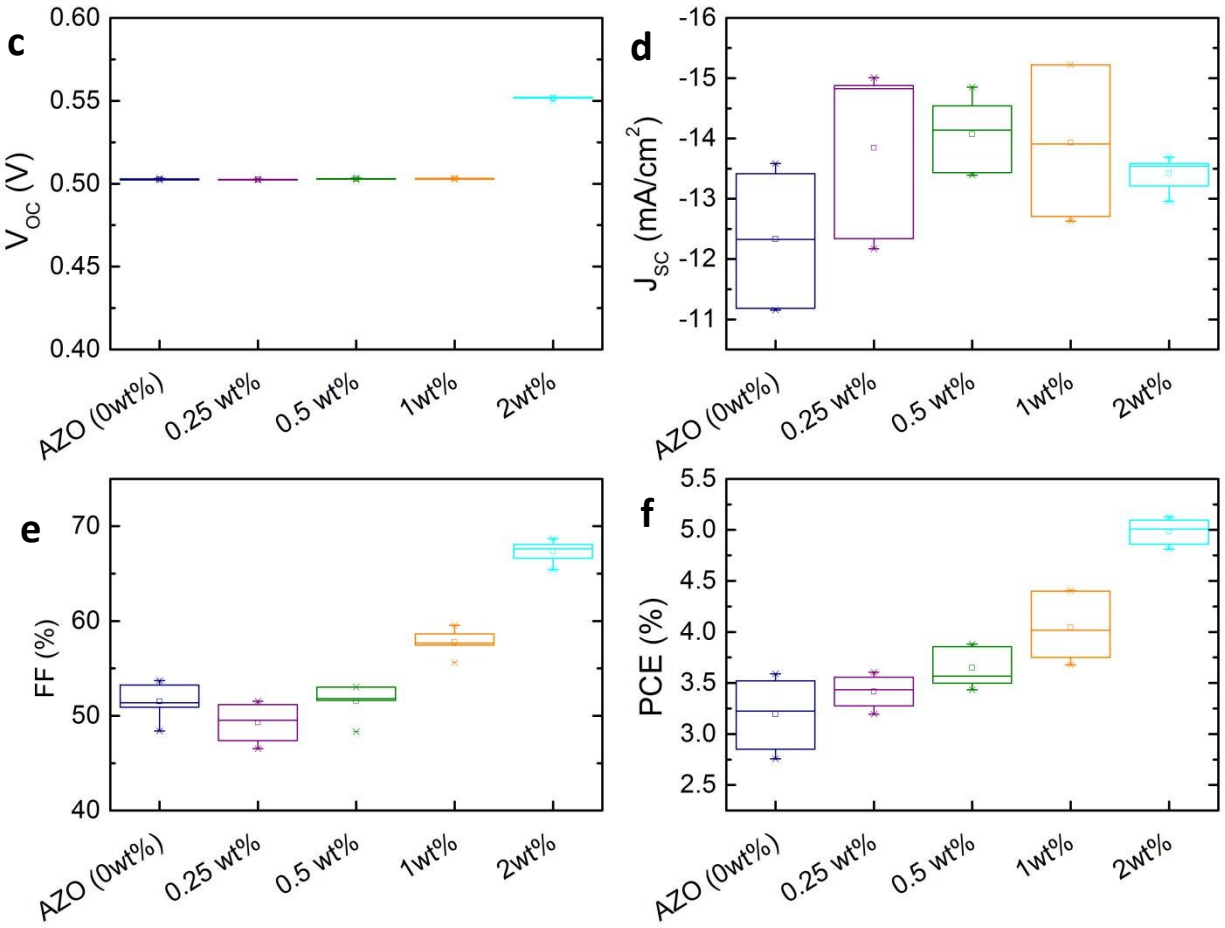

Figure S4. a) *j-V* characteristics of the OSCs (ITO/AZO/pDPP5T-2:$PC_{61}BM$:**Phen-NaDPO**/MoO_3/Ag) with different **Phen-NaDPO** contents in the ternary blend under illumination of an AM 1.5G solar simulator (100 mW/cm^2). b) Corresponding logarithmic plot of dark *j-V* characteristics. c-f) Photovoltaic parameters distribution of 5 solar cells; the boxes represent the 25-75% distribution range, and hollow squares represent the mean values.

Table S3. Summary of the *j-V* characteristics of inverted OSCs (ITO/AZO/pDPP5T-2:$PC_{61}BM$:Phen-NaDPO/MoO_3/Ag) with varying Phen-NaDPO content and inverted OSCs without and with the $Ba(OH)_2$ as reference* under simulated AM1.5 illumination (100 mW/cm^2).

Devices configuration	Phen-NaDPO (wt %)	V_{OC} (V)	J_{SC} (mA cm^{-2})	*FF* (%)	*PCE* (%) avg (best)
ITO/AZO/pDPP5T-2:$PC_{61}BM$:Phen-NaDPO/MoO_3/Ag	0	0.50	-12.40±1.02	51.73±2.53	3.25 (3.50)
	0.25	0.50	-13.90±1.10	50.00±3.01	3.50 (3.64)
	0.50	0.50	-14.02±0.76	52.50±1.73	3.74 (3.95)
	1.00	0.50	-13.91±1.07	58.63±1.07	4.04 (4.41)
	2.00	0.55	-13.50±0.49	67.31±1.92	5.07 (5.27)
ITO/AZO/pDPP5T-2:$PC_{61}BM$ /MoO_3/Ag		0.50	-12.31±1.02	53.90±1.96	3.17(3.33)
ITO/AZO/$Ba(OH)_2$/pDPP5T-2:$PC_{61}BM$ /MoO_3/Ag		0.55	-15.79±1.31	69.18±3.74	5.42(6.01)

* The data came from the reference [1].

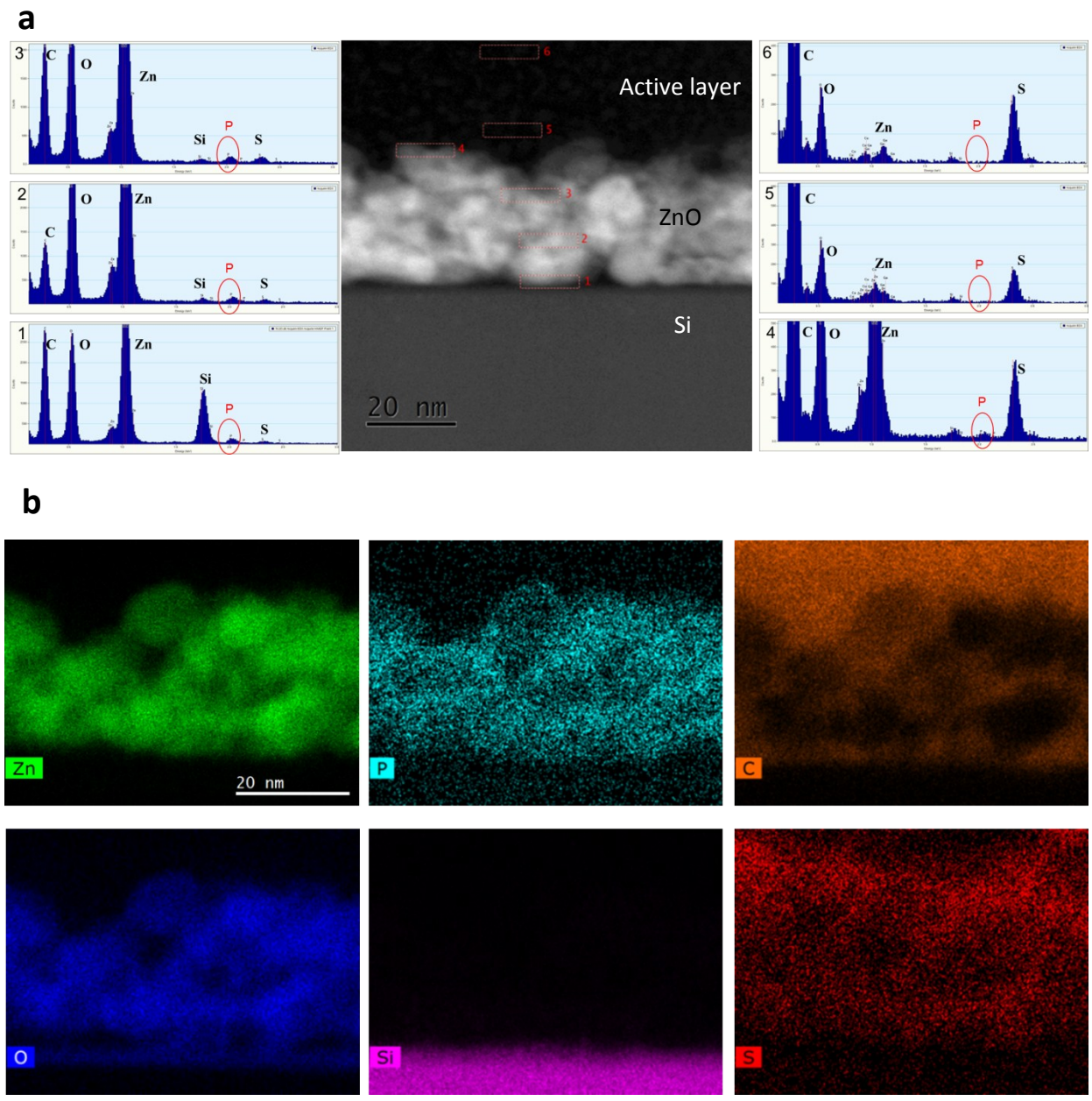

Figure S5. (a) Cross-sectional scanning transmission electron microscopy (STEM) image of the ZnO/active layer interface. EDX spectra outline the chemical composition at different locations. (b) STEM EDXS spectrum image showing the elemental distribution for Zn, P, C, O, Si and S.

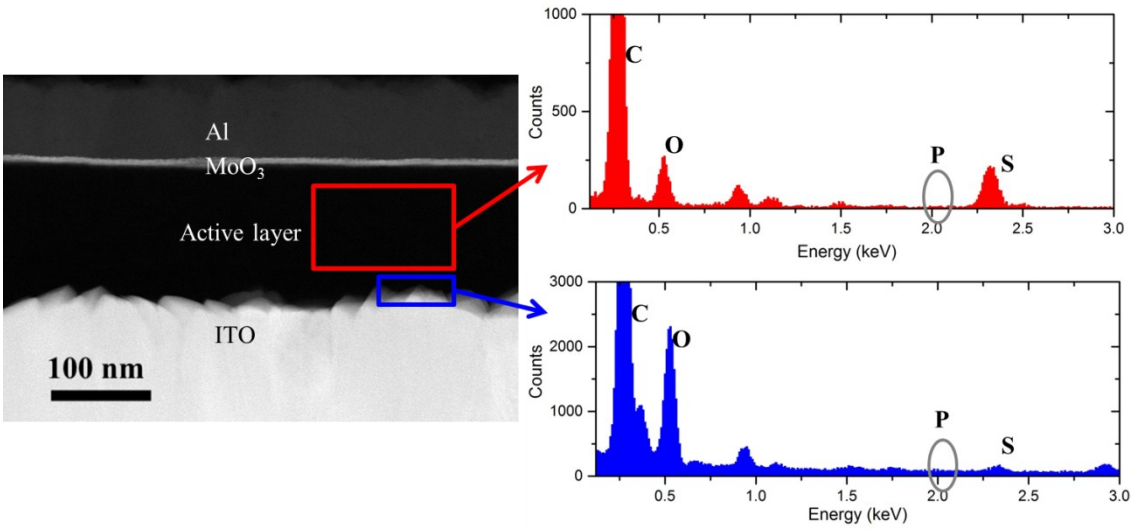

Figure S6. Cross-sectional scanning transmission electron microscopy (STEM) image showing the device architecture, ITO/"ternary" active layer/MoO_3/Al, (left). EDX spectra of "ternary" BHJ composites (right, red) and the interface between ITO and "ternary" blend active layer (right, blue).

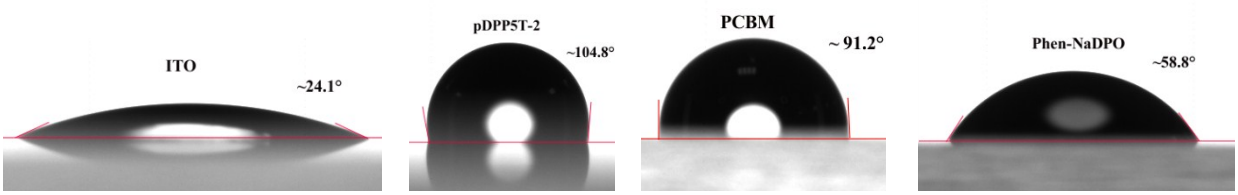

Figure S7. Photographs of water droplets on substrate surfaces coated with the ITO, pDPP5T-2, $PC_{61}BM$ and **Phen-NaDPO** films, respectively.

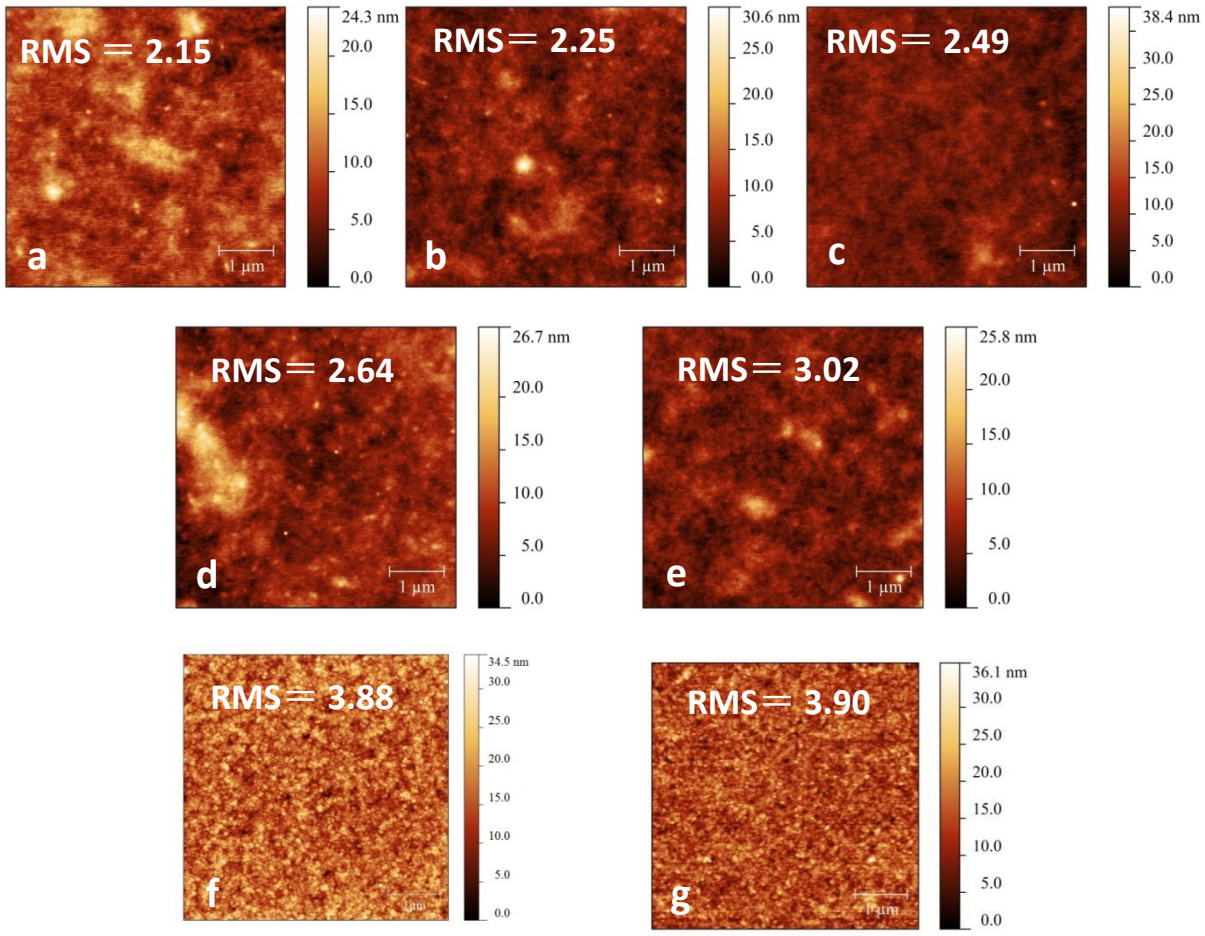

Figure S8. Surface topographic AFM images (size: 5.0 × 5.0 μm^2) of thin films: a) pDPP5T-2:$PC_{61}BM$; b) pDPP5T-2:$PC_{61}BM$:0.25 wt% Phen-NaDPO; c) pDPP5T-2:$PC_{61}BM$:0.50 wt% Phen-NaDPO; d) pDPP5T-2:$PC_{61}BM$:1.00 wt% Phen-NaDPO; e) pDPP5T-2:$PC_{61}BM$:2.00wt% Phen-NaDPO; f) ZnO layer; g) Phen-NaDPO (~8 nm) on the ZnO layer.

Reference

[1] H. Zhang, T. Stubhan, N. Li, M. Turbiez, G. J. Matt, T. Ameri and C. J. Brabec, *J Mater Chem A*, 2014, 2, 18917-18923.